

See discussions, stats, and author profiles for this publication at: <https://www.researchgate.net/publication/279728457>

Investigation on Transient Oscillation of Droplet Deformation before Conical Breakup under AC Electric Field.

ARTICLE *in* LANGMUIR · JULY 2015

Impact Factor: 4.46 · DOI: 10.1021/acs.langmuir.5b01642 · Source: PubMed

READS

17

7 AUTHORS, INCLUDING:



Xin Huang

China University of Petroleum

1 PUBLICATION 0 CITATIONS

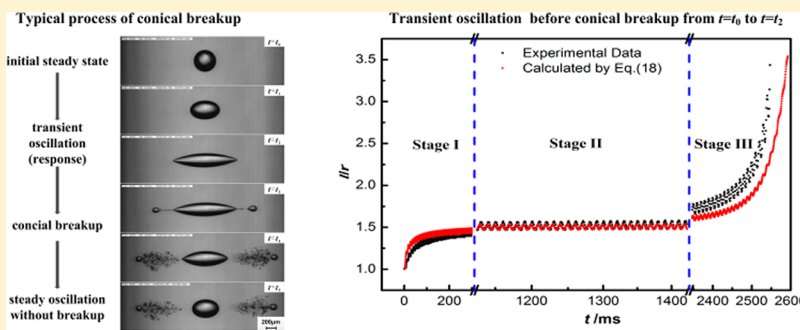
SEE PROFILE

Investigation on Transient Oscillation of Droplet Deformation before Conical Breakup under Alternating Current Electric Field

Haipeng Yan, Limin He,* Xiaoming Luo, Jing Wang, Xin Huang, Yuling Lü, and Donghai Yang

College of Pipeline and Civil Engineering, China University of Petroleum, No. 66 Changjiang West Road, Qingdao, Shandong 266580, China

Supporting Information



ABSTRACT: In this paper, the conical breakup of a water droplet suspended in oil under the alternating current (ac) electric field was experimentally studied with the help of a high-speed video camera. We observed three stages of transient oscillation of deformation characterized by deformation degree \tilde{t}^* before the conical breakup that were described in detail. Then a theoretical model was developed to find out the dynamic mechanisms of that behavior. Despite a very small discrepancy, good agreement between model predictions and experimental observations of the evolution of the droplet deformation was observed, and the possible reasons for the discrepancy were discussed as well. Finally, the stresses on the interface were calculated with the theoretical model and their influence on the dynamic behavior before the breakup was obtained. The differences between the droplet breakup mode of ac and direct current electric field are also discussed in our paper.

1. INTRODUCTION

The electrodehydration technology has been widely used in the petroleum industry for separating water-in-crude oil emulsions by applying an alternating current (ac) electric field to promote the coalescing efficiency. The vibration of droplets caused by the external electric field will set up wave disturbance of the oil film between droplets, which is helpful in accelerating the process of film thinning.¹ Moreover, greater deformation reduces the distance between the droplets pairs resulting in an increased attractive force. As a consequence, the velocity of each neighbor droplet increases as well as the possibility of electrostatic discharge between drops.^{2–4} However, for higher electric fields the capillary pressure may not afford the electric stresses and the droplet may undergo some form of breakup called electrodispersion resulting in significant efficiency decline.^{5,6} Therefore, further studies on the mechanisms of water droplets breakup under the ac electric field are necessary to enhance the efficiency of the commercial electrodehydrator.

A number of experimental and theoretical investigations have been carried out to elucidate the fundamentals and modes of droplet breakup under the external electric field. Assuming an ellipsoidal shape for the deformed interface, Taylor⁷ developed a model that describes the drop's steady-state deformation under the direct current (dc) electric field. With this model, he calculated the critical electric field intensity and the

corresponding aspect ratio of the onset of breakup. On the basis of a boundary integral formulation, Dubash and Mestel^{8,9} presented detailed numerical computations, and the results confirmed that the critical electric capillary number Ca_c is about 0.2 which was also obtained by Ha and Yang¹⁰ in their experiments. In addition, there have been a few studies^{10–14} on the modes of drop breakup. Ha and Yang¹⁰ carried out experiments on the breakup modes for Newtonian as well as non-Newtonian drops subjected to a uniform electric field, and the effects of rheological properties as well as resistivity and viscosity ratios were also investigated. Vizika and Saville¹¹ and Moriya et al.¹² observed two modes of breakup: one is the division of a drop into two lobes connected by a thin thread; the other is the tip streaming from a drop with pointed ends. However, they did not discuss the effects of Ca and the viscosity ratio on the dynamics of those phenomena. Motivated by the above problems, Karyappa et al.¹³ performed detailed experimental and numerical analysis. They investigated the effects of Ca and the viscosity ratio on different modes of drop breakup (axisymmetric shape prior to breakup (ASPB) and non-axisymmetric shape at breakup (NASB)) in dc field.

Received: May 5, 2015

Revised: July 2, 2015

Published: July 3, 2015

Despite numerous theoretical and experimental researches concerned on the drop breakup under the dc electric field, the dynamics of drop breakup in the ac electric field has received less attention. Wright et al.¹⁵ simulated the breakup of a viscous drop subjected to a time-dependent electric field. But the predictions of their model did not agree well with experimental measurements. Nishiwaki et al.¹⁶ studied the deformation of droplets in an alternating electric field of frequency 60 Hz for drops suspended in polymer solution. The critical field strength for droplet disintegration was achieved. Ye¹⁷ performed an experimental study on the deformation and breakup of drops subjected to the ac electric field. He explored the effects of electric field strength and frequency, the viscosity of oil phase and interfacial tension on the modes of breakup and the distribution of daughter droplets in detail. Otherwise the results were qualitatively explained and the dynamics of breakup was not clarified.

The dynamics of steady oscillation of drop deformation under ac electric field was investigated by a few researchers, but a further understanding of the transient process have heretofore been lacking. Torza et al.¹⁸ developed a theoretical model that predicts the dynamics of steady oscillation of drop deformation in the ac electric field. According to their model, the drop oscillates twice as fast as the electric field that was confirmed by Ye¹⁷ and Taylor.¹⁹ On the basis of the force balance analysis, Zhang et al.²⁰ and Gong et al.²¹ developed mathematical models, respectively, which both indicate the resonance frequency of drop deformation under the time-dependent electric field. Sherwood²² theoretically studied the transient oscillation of drop deformation and breakup in the creeping flow coupled with electric field. He reported different modes of breakup that depend on the physical properties of the drop and host fluids.

Besides the investigations of free drop mentioned above, the oscillation of the pendant and sessile drops caused by the time-dependent electric field also draw many attentions.^{23–27} Basaran et al.²³ studied the oscillations of inviscid, conducting drops subjected to a step change electric field. The effect of the field strength was explored by theoretical and experimental analysis. They found that the drop would oscillate under small field strength. When the field strength is large enough, the drops do not oscillate any more but become unstable by issuing jets from their tips. Yeo et al.²⁴ found that the oscillation of a pendant drop under ac electric field, unlike the dc electric field, shows resonance, and drops are ejected from the resonating meniscus. The dynamic deformation of a sessile water drop in oil under different waveforms of electric field was studied by Gunnar et al.²⁵ The surface oscillations were observed and modeled as damped oscillator. They believed that the oscillations could explain the breakup of water droplets. A systematic investigation of the transient oscillations of Taylor cones of an anchored hemispherical meniscus subjected to a step change electric field was performed by Deng and Gomez.²⁶ The transient response of Taylor cones was explained by a meniscus damping model. Jonathan et al.²⁷ developed a novel technique for on-demand injection of charge-free conductivity droplets utilizing the transient deformation of a water meniscus under high electric field. Though the droplet used in these researches was not free, their theories and experimental results have been very helpful in the investigations on the dynamics of a free drop breakup in the ac electric field.

With the help of high speed photography, we observed two modes of droplet breakup under the high voltage ac electric field: the conical breakup¹⁷ and the filamentous breakup. In this

paper, we aim to discuss the dynamics of the droplet deformation before the conical breakup under the ac electric field. First, we described the typical process of the conical breakup in detail, especially the law of deformation degree l^* before the breakup happens. Afterward, a theoretical model was developed to explore the dynamics mechanism. Then the numerical and experimental results were compared with each other, and the possible reasons for the discrepancy were discussed. Finally, we expounded the dynamics of oscillatory deformation before the conical breakup by calculating the stresses on the interface.

2. EXPERIMENTAL SETUP AND MATERIALS

2.1. Experimental Setup. The experimental system and cell used in this study are similar to the ones used by Yan et al.²⁸ and are depicted in Figures 1 and 2. The cell was made with Perspex so that

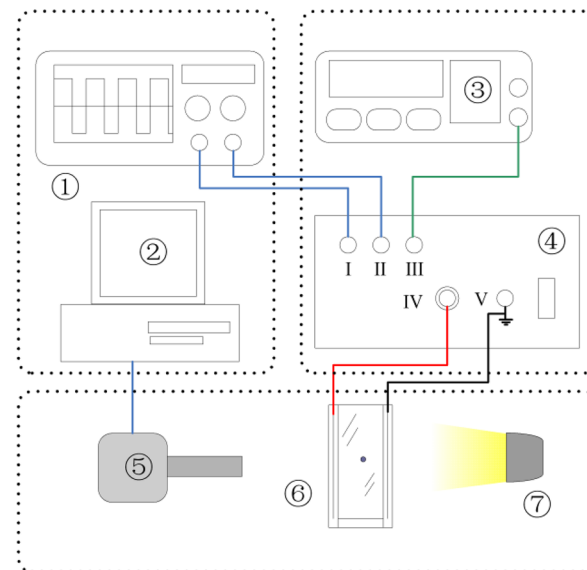


Figure 1. Apparatus of the experimental instrument. ① Oscilloscope; ② PC; ③ arbitrary waveform generator; ④ high voltage source; ⑤ high-speed digital video camera; ⑥ test cell; and ⑦ LED light source. I: voltage monitor port. II: current monitor port. III: signal input. IV: high voltage output. V: grounded.

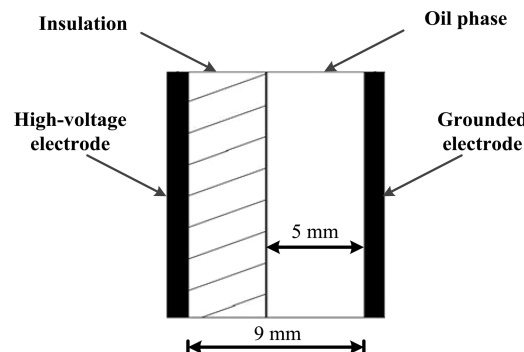


Figure 2. Schematic diagram of experimental cell.

the droplet breakup process could be recorded by a high-speed digital video camera (NAC Hotshot 1280) equipped with a lens (Mitutoyo 5× objective with a tube made by Pomeas). The camera was used with a frame rate of 1000 fps, and the resolution was 1280 × 512 pixels. A self-made LED was used for lighting without changing the oil temperature in the cell.

Table 1. Properties of Oil and Water at 25°C^a

phase	viscosity/mPa·s	relative dielectric constant	conductivity/S·m ⁻¹	interfacial tension/mN·m ⁻¹
continuous	950	2.26	10 ⁻¹²	41.4
dispersed	1.72	82	4.6 × 10 ⁻⁴	

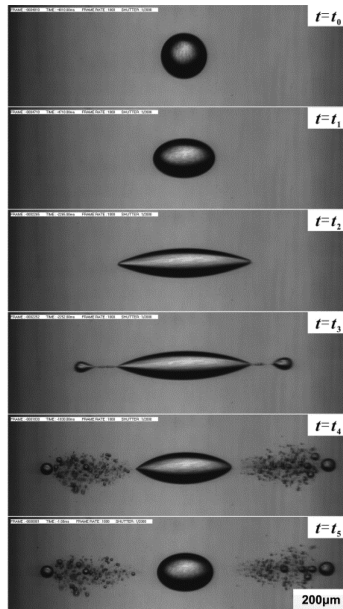
^aThe room temperature was controlled at 25°C throughout the experiment.

initial steady state

transient oscillation (response)

conical breakup

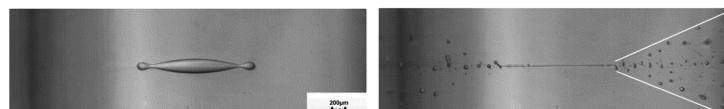
steady oscillation without breakup



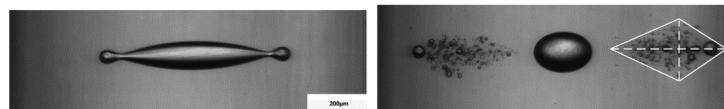
(a)

Before breakup

Beakup



(i) DC electric field



(ii) AC electric field

(b)

Figure 3. (a) Typical process of conical breakup of a water droplet subjected to ac electric field. The radius of the droplet is about 190 μm . The amplitude value of applied ac electric field E_0 was about 1810 $\text{kV}\cdot\text{m}^{-1}$, the frequency was 50 Hz. The frame rate was 1000 fps. Scale bar: 200 μm . (b) Comparison of the similar breakup mode occurred under the (i) dc electric field; (ii) ac electric field.

The cell had two polished stainless steel electrodes with dimensions of 40 mm × 30 mm (about 2 mm in thickness). The Perspex block having a thickness of approximate 4 mm was attached to the high voltage electrode, which was connected to a high voltage source (Trek 20/20C). The high voltage source was fed by an arbitrary waveform generator (Rigol 2041A, Beijing RIGOL Technology Co., Ltd.) that provided a sine waveform. The bare metal on the right side of cell was a grounded electrode. The voltage and current were monitored by oscilloscope (TDS2002B, Tektronix). The electric field strength E was calculated by eq 1

$$E = E_0 \sin \omega t \quad (1)$$

where the amplitude value E_0 was about 1810 $\text{kV}\cdot\text{m}^{-1}$ and $\omega = 2\pi f$ was the angular frequency of the field with $f = 50$ Hz. Feng et al.²⁹ suggested that under strong electric field the electrical breakdown of dielectric layer would happen. Compared to their research, the electric field strength used in this paper was relatively high. However, as the droplet was smaller which was relatively far from the electrode (the magnitude of radius of droplet was 10^{-1} mm and that of the distance of electrodes was 1 mm) and could not contact the electrodes or the insulation even after breakup, electrical breakdown would not happen in our case.

2.2. Materials. White oil was used as the continuous phase (obtained from YanChang Petrochemical Product Co., Ltd., Beijing), and distilled water as the dispersed phase (provided by College of Chemical Engineering, China University of Petroleum). Liquid viscosity was measured using rheometer (Anton Paar GmbH, Austria). The conductivity was measured using a conductivity meter, Model DDS-11A from INESA Scientific Instrument Co., Ltd. for dispersed phase and Model GD29YX1154B from China Electric Apparatus Research Institute Co., Ltd. for continuous phase. Interfacial tension was measured by K10-ST from Kruss GmbH. The dielectric constant

of the pure liquids was obtained from the literature. The properties are presented in Table 1.

The grounded micropipette (Brand GmbH & CO.KG, Germany) was used to produce a small charge-free droplet. It could be considered to be subjected to a uniform electric field when introduced at the middle of the cell. As the drop deformed into a prolate spheroidal shape under our conditions, the deformation could be characterized by the deformation degree l^* calculated by eq 2 where l and r are the semimajor axis and radius of the drop, respectively. l is the drop length parallel to the electric field, and r is the original radius of droplet (see Figure 5). The semimajor l and radius r were determined by software. The pixel length was 2.8 μm .

$$l^* = \frac{l}{r} \quad (2)$$

3. EXPERIMENTAL RESULT

3.1. Conical Breakup of a Water Droplet in Oil under ac Electric Field. The whole process of conical breakup for an isolated droplet exposed to ac electric field consists of multiple sequential processes as illustrated in Figure 3a. It is a procedure from a static spherical shape in the beginning to a steady-state oscillation after the unsteady conical breakup.

Before $t = t_0$, no electric field was applied, so the interfacial tension would keep the water drop spherical ($r \approx 190 \mu\text{m}$). At $t = t_1$, shortly after the electric field was applied the drop deformed into an ellipsoidal shape due to the electrostatic pressure (F_e) on the surface and elongated in the direction of the electric field. From t_1 to t_2 , the ends gradually developed into cones with increasingly sharper tips until the critical conditions were reached, and that is why we call it conical breakup. At $t = t_3$, the lobes formed at the two ends, and they moved off quickly away from the mother drop. Because of the

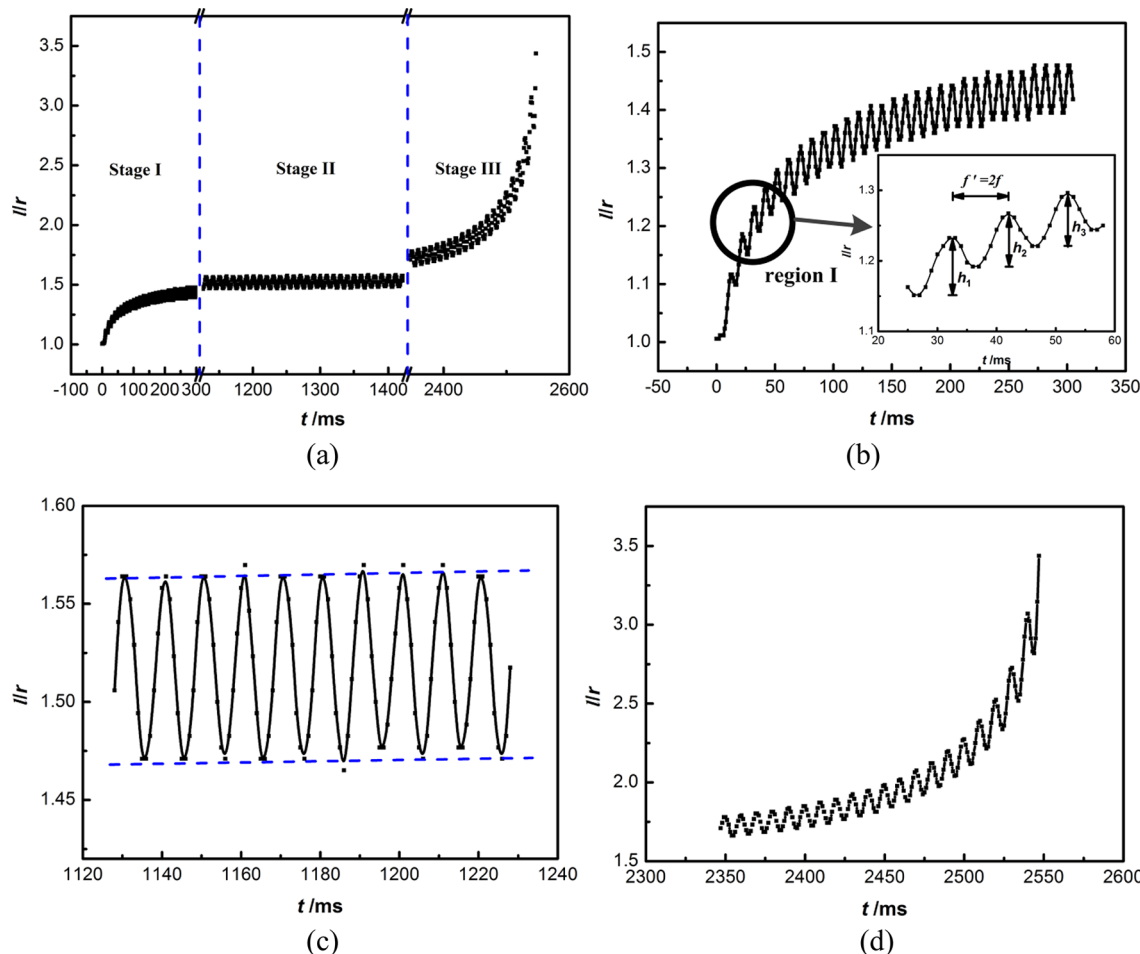


Figure 4. Transient oscillation of a water droplet in oil under ac electric field before conical breakup. The evolution of deformation degree l^* could be divided into three stages that are presented in plots (b–d), respectively. Inset of plot (b) shows l^* versus t of the region I circled by bold solid line. The electric frequency $f = 50$ Hz, and the electric field strength $E_0 = 1810$ kV·m $^{-1}$.

variation of the electric field, the cone retracted. Consequently, a thread usually appeared between the lobe and the mother drop and then it broke into multiple droplets when the Plateau-Rayleigh instability was met. This sequence of drop breakup might last for a period until the conditions of the mother drop did not meet that of breakup any more at $t = t_4$. Thereafter, the droplet retracted to ellipsoidal shape and oscillated at steady frequency that was about as twice as the electric field.

It is a bit similar to Karyappa's observation of lobes in ASPB and charged lobe disintegration mode in NASB.¹³ However, some differences can be found between the two breakup modes: (1) According to Karyappa's report,¹³ for the breakup under the dc electric field, a dimple forms at the electrode-facing pole of the first lobe, and then the dimple grows creating a crater of the sort with an outer ring. However, for the breakup under the ac electric field, we did not observe the dimple. Moreover, the first lobe kept spherical shape all the time. (2) The distribution of the smaller drops is different. As shown in Figure 3b, the distribution was radial in the dc electric field that was a combination of two isosceles triangles in the ac electric field. These differences may be caused by the type of electric field, namely under the dc field the electric stress on the surface is almost unchanged, while under the ac field it is changed all the time.

According to the experimental and numerical results,^{8,9,13,14} in dc electric field the charged lobes could possibly break into several smaller droplets after the lobes detach from the mother drop resulting from the Rayleigh-like instability^{8,9} and/or the Saffman-Taylor instability.¹³ Then the smaller droplets are driven by the electrostatic force and

move toward the adjacent electrode. This is similar to the effect of electrophoresis. The direction of the tensile stress on the edge of the outer ring is at a certain angle to the plane, thereby the smaller droplets generating from the edges would possibly move along the radial direction. Finally, the radial distribution of smaller droplets would be observed under dc electric field. As to the distribution of smaller drops under ac electric fields, the reason may lie in the local electric field between the conical end of the mother drop and the first daughter drop. In order to reach the balance, the smaller droplets staying at certain positions between the mother and the first daughter drop are likely to distribute along the electric field lines (the cluster of electric field lines is similar to the combination of two isosceles triangles).

3.2. Transient Oscillation before Conical Breakup.

As illustrated in Figure 4a, the transient oscillation of a droplet in oil under ac electric field before conical breakup (from about $t = t_0$ to $t = t_2$ in Figure 3a) can be divided into three stages.

In stage I (see Figure 4b), the deformation degree of the droplet increases rapidly, but the amplitude of the periodic deformation h decreases gradually to a stable value (about 0.1) at the end of stage I (see Figure 4b). Moreover, as shown in the inset of Figure 4b the deformation degree oscillates at a fixed frequency f' which is about twice of electric field, that is, $f' \approx 2f$. In stage II and III, the oscillation frequency of deformation is also about twice as that of electric field (see Figure 4c, d). However, in stage II the increasing rate of the mean deformation degree is very slow while the amplitude of the time periodic deformation is almost the same until the deformation entered stage III in which l^* increases rapidly again.

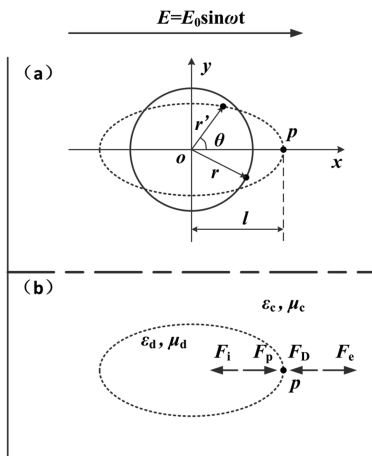


Figure 5. Schematic of a drop under ac electric field. (a) Coordinate system for analytical theory; (b) stress analysis of the droplet.

In the following section, the transient oscillation of a droplet in oil under ac electric field before conical breakup (from about $t = t_0$ to $t = t_2$ in Figure 3a) is explained by the electrohydrodynamic analysis on the point p (see Figure 5).

4. THEORETICAL SECTION

We consider a spherical drop with radius r that is neutral in charge and is suspended in an immiscible fluid subject to an ac electric field. In this paper, the theoretical model is based on the following assumptions:

(1) The electric field strength E varies with time t according to eq 1 and its direction is shown in Figure 5. The ratio of the radius of droplet to the height of the electrodes $H \ll 1$ so that the electric field can be considered as uniform;

(2) The Bond number $Bo = \Delta \rho g r^2 / \gamma \ll 1$, so the gravitational effects are negligible;

(3) The dielectric constants ϵ_c and ϵ_d and the ohmic resistivities Γ_c and Γ_d of the continuous phase and drop are respectively independent of the frequency of electric field f ;

(4) The ratio of conductivity of the continuous phase to that of drop $R \approx 0$;

(5) The interface is surfactant free, which means that the interfacial tension between the drop and the continuous phase is constant and independent of the deformation.

The stresses on the point $p(\theta = 0)$ in Figure 5 are analyzed, and then the motion of p is obtained according to Newton's second law. Because the gravity and buoyancy are negligible, the point p is mainly subjected to the electric stress (F_e), radial hydrodynamic stress (F_D), additional pressure (F_p), and capillary pressure (F_i).

4.1. Electric Stress F_e at the Drop Interface. The electric stress F_e at the drop interface is a vector sum of the normal component F_{er} and transverse component $F_{e\theta}$.³⁰ On the basis of our assumption, $R \approx 0$ and $\theta = 0$ at the point p , according to the derivation by Torza et al.¹⁸ the transverse component $F_{e\theta} = 0$ while the normal component F_{er} could be written as

$$F_e = F_{er} = F_{erv} + F_{erT} \quad (3a)$$

$$F_{erv} = \frac{9}{4} \epsilon_0 \epsilon_c E_0^2 \frac{1 + \tau^2 \omega^2 q(q - 1)^2}{1 + \tau^2 \omega^2 (q + 2)^2} \quad (3b)$$

$$F_{erT} = \frac{9}{4} \epsilon_0 \epsilon_c E_0^2 [\operatorname{Re}(F_r^* e^{i2(\omega t - \frac{\pi}{2})})] + w_T \quad (3c)$$

where $\tau = \epsilon_0 \epsilon_c \Gamma_d$, $q = \epsilon_d / \epsilon_c$ and w_T , F_r^* and A are given by

$$w_T = \frac{9}{8} \epsilon_0 \epsilon_c E_0^2 (q - 1) [A^2 e^{i2(\omega t - \frac{\pi}{2})} + \hat{A}^2 e^{-i2(\omega t - \frac{\pi}{2})}] \quad (3d)$$

$$F_r^* = A^2 (5 - 2q) - 2A + 1 \quad (3e)$$

$$A = \frac{i\tau\omega}{1 + i\tau\omega(q + 2)} \quad (3f)$$

with \hat{A} being the complex conjugate of A .

It is found that $\tau \approx 0$ under the assumption, so the eqs 3b and 3c could further reduce to

$$F_{erv} = \frac{9}{4} \epsilon_0 \epsilon_c E_0^2 \quad (4a)$$

$$F_{erT} = -\frac{9}{4} \epsilon_0 \epsilon_c E_0^2 \cos 2\omega t \quad (4b)$$

Finally, F_e could be given by

$$F_e = F_{erv} + F_{erT} = \frac{9}{4} \epsilon_0 \epsilon_c E_0^2 (1 - \cos 2\omega t) \quad (5)$$

4.2. Radial Hydrodynamic Stress F_D . Radial hydrodynamic stress F_D is the difference between the radial pressure outside (p_{cr}) and inside (p_{dr}) the drop due to the fluid motion that is caused by (i) $F_{e\theta}$, the transverse component of electric stress, and (ii) F_{erT} , which induces oscillation of the drop surface and hence an oscillating flow. The former is referred to as F_D^I , the latter F_D^{II} . The total radial hydrodynamic stress is the sum of F_D^I and F_D^{II}

$$F_D = p_{cr} - p_{dr} = F_D^I + F_D^{II} \quad (6)$$

As mentioned above, $F_{e\theta} = 0$, so $F_D^I = 0$. Substituting $R \approx 0$ and $\theta = 0$ into corresponding equations given by literature¹⁸ yields on reduction

$$F_D^{II} = -\frac{3}{2} \lambda_2 k \frac{\epsilon_0 \epsilon_c E_0^2}{\sqrt{1 + k^2 \lambda_2^2}} \cos(2\omega t + \varphi) \quad (7a)$$

$$\tan \varphi = \frac{1}{k \lambda_2} \quad (7b)$$

$$k = \frac{\mu_c \omega r}{\gamma} \quad (7c)$$

$$\lambda_2 = \frac{(19\lambda + 16)(2\lambda + 3)}{20(\lambda + 1)} \quad (7d)$$

where λ is the ratio of viscosity of the drop to that of continuous phase $\lambda = \mu_d / \mu_c$ and γ is the interfacial tension.

The velocity at p eq 8 could be derived from the equation of the drop surface that was given by Torza et al.¹⁸

$$\frac{dl}{dt} = \frac{8}{3} r \omega \operatorname{Re}(iH^* e^{2i\omega t}) \quad (8)$$

On the basis of our assumptions

$$\operatorname{Re}(iH^* e^{2i\omega t}) = \frac{9 \epsilon_0 \epsilon_c E_0^2 r}{32 \gamma} \frac{1}{\sqrt{1 + k^2 \lambda_2^2}} \times \cos(2\omega t + \varphi) \quad (9)$$

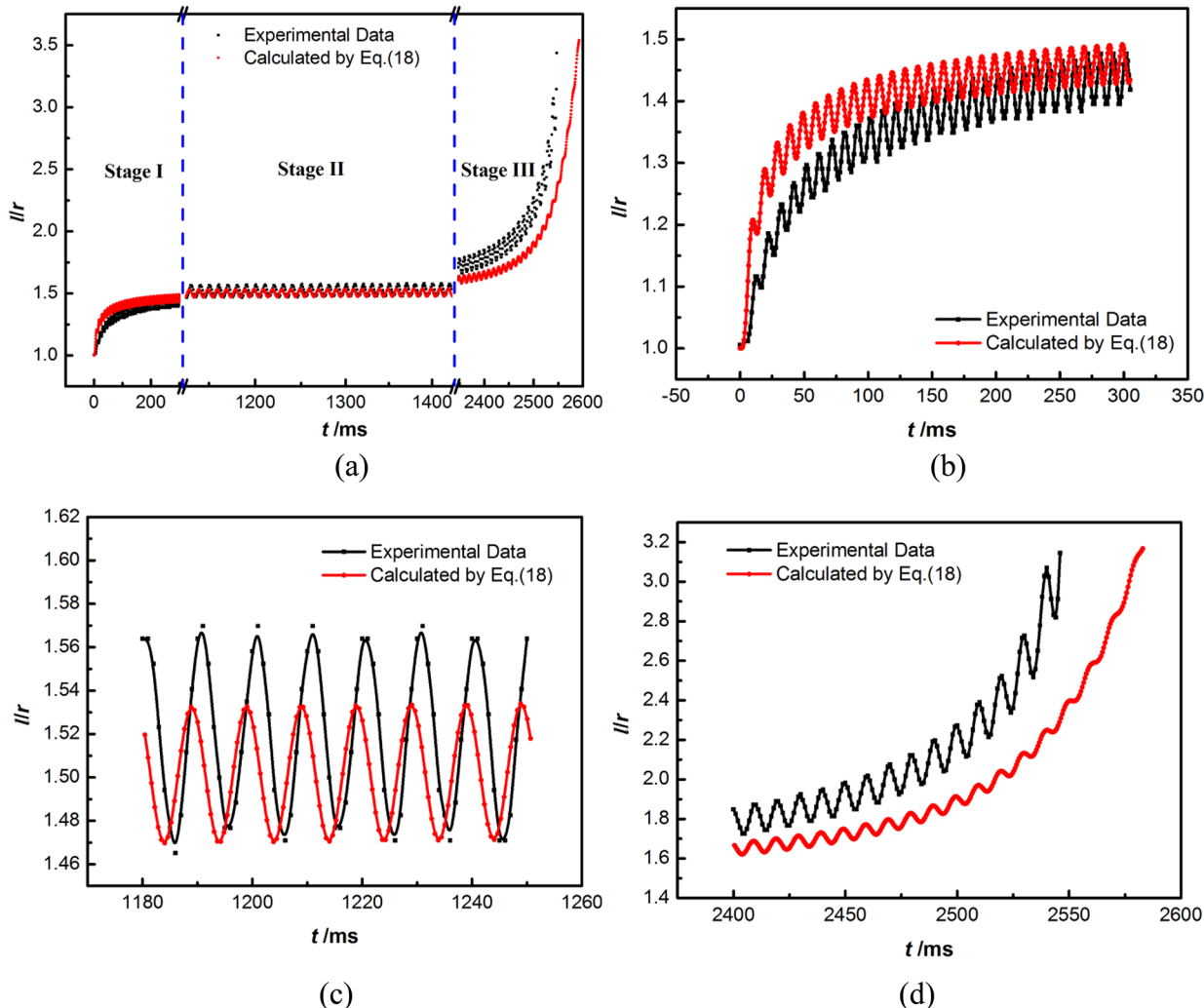


Figure 6. Transient oscillation of a water droplet in oil under ac electric field before conical breakup from the experiment (black solid line) and calculation of the theoretical model (red solid line). The three stages of evolution of deformation degree before the conical breakup are presented in plots (b–d), respectively. The electric frequency $f = 50$ Hz, and the electric field strength $E_0 = 1810$ kV·m $^{-1}$.

Imposing eq 9 on eq 8 and then comparing the simplification equation with eq 7 yields

$$F_D^{II} = -\frac{2\mu_c \lambda_2}{r} \frac{dl}{dt} \quad (10)$$

Substituting eq 10 into eq 6 we obtain

$$F_D = F_D^I + F_D^{II} = F_D^{II} = -\frac{2\mu_c \lambda_2}{r} \frac{dl}{dt} \quad (11)$$

4.3. Capillary Pressure F_i .

Capillary pressure F_i is given by

$$F_i = -2\gamma \left(\frac{1}{r_1} + \frac{1}{r_2} \right) \quad (12)$$

with r_1, r_2 being the principal radii of curvature. According to the equation which describes the shape of drop interface put forward by Troza et al.,¹⁸ the capillary pressure could be reduced to eq 13 in our case

$$F_i = -2\gamma \left(\frac{1}{r_1} + \frac{1}{r_2} \right) = -\gamma \left(\frac{8}{l} - \frac{6r}{l^2} \right) \quad (13)$$

4.4. Additional Pressure F_p .

In the absence of an electric field, the drop with radius r could keep its spherical shape due

to the capillary pressure against the additional pressure F_p , which is given by the Young–Laplace equation

$$F_p = \frac{2\gamma}{r} \quad (14)$$

The additional pressure F_p could be treated as a constant during the evolution of deformation.

4.5. Boundary Conditions and Nondimensionalization. Substituting eqs 5, 11, 13, and 14 into the Newton's second law eq 15, we obtain the motion of p described by eq 16

$$C_m \frac{d^2l}{dt^2} = F_e + F_D + F_p + F_i \quad (15)$$

$$\frac{d^2l}{dt^2} + \frac{2\mu_c \lambda_2}{C_m r} \frac{dl}{dt} + \frac{\gamma}{C_m} \left(\frac{8}{l} - \frac{6r}{l^2} \right) = \frac{9\epsilon_0 \epsilon_c E_0^2}{4C_m} (1 - \cos 2\omega t) + \frac{2\gamma}{C_m r} \quad (16)$$

where C_m is defined as a constant corresponding to areal density of the interface, kg·m $^{-2}$. The boundary conditions are taken to be

$$l = r, \quad \frac{dl}{dt} = 0 \text{ at } t = 0 \quad (17)$$

To nondimensionalize eq 16, we construct the deformation degree $l^* = l/r$, relevant time $t^* = t/(\rho_d r^3/\gamma)^{0.5}$, relevant angular frequency $\omega^* = \omega(\rho_d r^3/\gamma)^{0.5}$ and $C_m = C_m' \rho_d r$, where ρ_d is the density of the water drop, $\rho_d = 1000 \text{ kg}\cdot\text{m}^{-3}$. With the four nondimensional variables, eq 16 can be transformed into

$$\begin{aligned} \frac{d^2l^*}{dt^{*2}} + \frac{2\lambda_2}{C_m'} \cdot Oh \frac{dl^*}{dt^*} + \frac{2}{C_m'} \left(\frac{4}{l^*} - \frac{3}{l^{*2}} \right) \\ = \frac{9}{4} \frac{Ca}{C_m'} (1 - \cos 2\omega^* t^*) + \frac{2}{C_m'} \end{aligned} \quad (18)$$

with

$$l^* = 1, \quad \frac{dl^*}{dt^*} = 0 \text{ at } t^* = 0 \quad (19)$$

where

$$Oh = \frac{\mu_c}{\sqrt{\rho_d r \gamma}}, \quad Ca = \frac{\epsilon_0 \epsilon_c r E_0^2}{\gamma} \quad (20)$$

In our case, $Oh = 10.74$ and $Ca = 0.3$ which is bigger than the critical value obtained by investigations of breakup in dc field.

It is found that eq 18 is similar to the model of forced vibration with damping. As shown in eq 18, the oscillation is significantly affected by three dimensionless numbers named (i) the Ohnesorge number (Oh), which relates the viscous forces to inertial and surface tension forces, (ii) the electric capillary number Ca , which relates the electric stress to the capillary stress, and (iii) the ratio of viscosity of the drop to that of continuous phase λ . Besides, when solving the model we found that C_m' is also important to the transient oscillation before the conical breakup by its damping on the amplitude. However, we have not obtained the method for calculation of C_m' yet. But with $C_m' = 265$ obtained by trial and error, there is a good correspondence between the computational result and the experimental one (see Figure 6a).

4.6. Results and Discussion. By taking the related physical and electrical parameters (Table 1) into eq 18, the dynamic evolution of l^* as well as the stresses on the interface versus time could be calculated through the fourth-order Runge–Kutta Method.

Figure 6 shows a plot of l^* calculated by eq 18 that is compared to the experimental result before the conical breakup. Overall, the two curves are in close agreement (see Figure 6a, the error is within 9% of the experimental result) but some deviations could be found in the three stages as depicted in Figure 6b–d.

(i) There is a slight time difference between the model predictions and the experimental results. It is most likely caused by the polarization effect of insulation that was not taken into account in the model or due to the time difference between the moments when we triggered the high speed video for the recording and when the electric field was applied in our experiments.

(ii) The model predicts lower amplitude of oscillation. The value of C_m' might be responsible for this deviation. The bigger C_m' would cause more damping on the amplitude, just like the influence of mass on the vibration with damping.

(iii) At stage III, the experimental results are obviously greater than calculated from the theory. The discrepancy becomes more pronounced as the droplet reaches the breakup point. This is similar to the findings of Torza et al.¹⁸ who

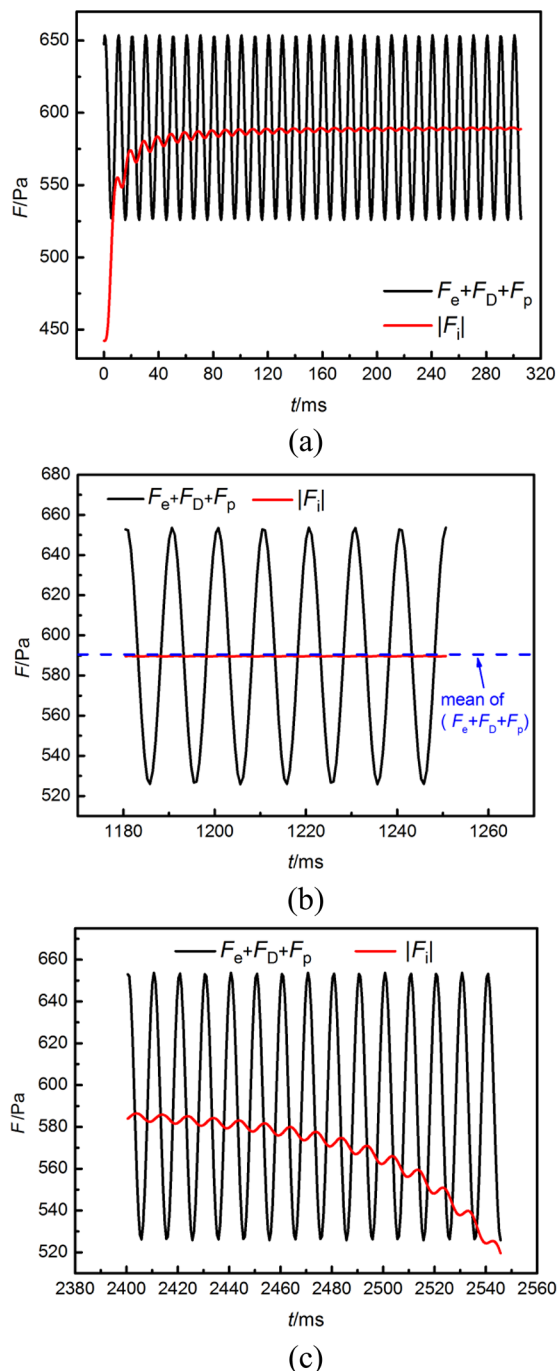


Figure 7. Plots of stresses on the interface versus time for the three stages before the conical breakup calculated by the theoretical model. (a–c) Plots of relationship between F_0 (sum of F_e , F_D , and F_p , black solid line) and the absolute value of F_i (red solid line) in each stage. The electric frequency $f = 50 \text{ Hz}$, and the electric field strength $E_0 = 1810 \text{ kV}\cdot\text{m}^{-1}$.

suggested that the possible reasons may be (1) limitations in the electric model assumed in the theory, (2) effects of space charges that are ignored in the electric model, and (3) effects due to the diffuse ionic layers at the interface.

Figure 7 shows plots of the stresses on the interface versus time for the three stages before the breakup. For the sake of contrastive analysis, we define F_0 as the sum of F_e , F_D , and F_p . The dynamic evolution of F_0 and $|F_i|$ (absolute value of F_i) is discussed in detail below.

Figure 7a–c shows the relationship between F_0 and $|F_i|$ in the three stages, respectively. In all the three stages, the amplitude of oscillation of F_0 is almost the same, while that of $|F_i|$ is significantly different. At the very beginning of stage I (Figure 7a), F_0 is much greater than $|F_i|$, as a consequence the droplet deforms quickly. Owing to the increase of the curvature of p with the deformation, $|F_i|$ experiences a rapid increase that causes the decrease of total stress and the reduction of the increasing rate of deformation. At the end of stage I, the oscillation amplitude of $|F_i|$ is declined gradually. In stage II (Figure 7b), compared with F_0 , the oscillation amplitude of $|F_i|$ is extremely small and the mean of $|F_i|$ approaches to that of F_0 . It could be imaged that the total stress ($F_0 - |F_i|$) on the interface oscillates around zero in this stage. This is probably the reason for the slow and almost undamped deformation in stage II. In stage III (Figure 7c), the oscillation amplitude of $|F_i|$ is increasing while $|F_i|$ goes down. As a consequence, the deformation rapidly goes up again.

It should be noted that in stage III the curvature of p is decreasing with the increasing deformation. In order to explore the reasons, the function $(8/l - 6r/l^2)$ with $r \approx 190 \mu\text{m}$ is plotted in Figure 8. Figure 8 shows that with the increase of l ,

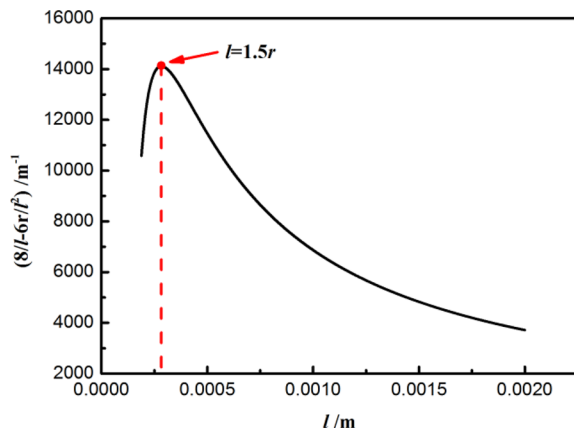


Figure 8. Plot of function $(8/l - 6r/l^2)$ with $r \approx 190 \mu\text{m}$ versus l which is the length of Op.

$(8/l - 6r/l^2)$ increases first and then decreases at $l = 1.5r$. That is to say with $\text{Ca} = 0.3$ if $l^* > 1.5$, which is almost the mean of the time periodic deformation of stage II, the breakup may occur. However, according to the numerical analysis in the dc electric field carried out by Dubash et al.,⁸ when $\text{Ca} = 0.3$, the droplet would breakup quickly without the slow deformation stage that appears only when Ca is close to its critical value (l^* is also around 1.5 in the slow deformation stage under the dc electric field). Therefore, it might be inferred that the ac electric field postpone the breakup of droplet.

In summary, the relationship between F_0 and F_i plays an important role in the evolution of drop deformation before the onset of conical breakup.

5. CONCLUSIONS

The transient oscillation of a water droplet suspended in oil before the conical breakup under the ac electric field was studied by experiment and numerical calculations. We described the whole dynamic process of the conical breakup in detail, especially the law of changes in parameter of deformation degree l^* . We observed that the transient oscillation of

a droplet before its conical breakup can be divided into three stages. Their features were described in detail. In stage I and III, the droplet undergoes rapid deformation. However, in stage II it experiences a period of slow deformation without damping.

To figure out the dynamics of the transient oscillation, we developed a theory model that is similar to the model of forced vibration with damping by analysis of electric stress (F_e), radial hydrodynamic stress (F_D), additional pressure (F_p), and capillary pressure (F_i). Using the fourth-order Runge–Kutta Method, the dynamic evolution of l^* as well as the stresses on the interface versus time were calculated. There is a good correspondence between the model predictions and the experimental results. Also, the error is within 9%. The reasons for the deviations have been discussed in the paper.

The dynamics of the transient oscillation before the breakup have been interpreted. It is found that the oscillation amplitude of F_0 is almost the same but that of F_i is significantly different. The reason why the curvature of p decreased with the increasing deformation at stage III was explored as well.

The equation for C_m' will be developed in a future study. Besides, it could be inferred from eq 18 that the Ohnesorge number Oh , the electric capillary number Ca , the interfacial tension, and the ratio of viscosity are all very important to the transient process. Therefore, further investigations are necessary to explore the effects of these parameters, especially the interfacial tension that was defined as a constant in this paper. The interface of oil and water containing the surfactant or the polymer would become a viscoelastic interfacial film, whose interfacial tension is not a constant, but rather a function of the droplet shape. The transient oscillation might be considerably different in that case, which we will focus on in a future study.

■ ASSOCIATED CONTENT

S Supporting Information

Video shows the typical process of conical breakup of a water droplet subjected to ac electric field. The radius of the droplet is about $190 \mu\text{m}$. The amplitude value of applied ac electric field E_0 was about $1810 \text{ kV}\cdot\text{m}^{-1}$, the frequency was 50 Hz. (The video contains every frame of the original recordings at 1000 fps.) The Supporting Information is available free of charge on the ACS Publications website at DOI: 10.1021/acs.langmuir.5b01642.

■ AUTHOR INFORMATION

Corresponding Author

*E-mail: upcyhp@163.com. Tel: +86-532-86983578.

Notes

The authors declare no competing financial interest.

■ ACKNOWLEDGMENTS

The work is supported by National Natural Science Foundation of China (Grant 51274233) and Natural Science Foundation of Shandong Province (Grant ZR2014EEM045).

■ REFERENCES

- Brown, A. H.; Hanson, C. Effect of Oscillating Electric Fields on Coalescence in Liquid–Liquid Systems. *Trans. Faraday Soc.* **1965**, *61*, 1754–1760.
- Eow, J. S.; Ghadiri, M. Drop–Drop Coalescence in an Electric Field: the Effects of Applied Electric Field and Electrode Geometry. *Colloids Surf, A* **2003**, *219*, 253–279.
- Eow, J. S.; Ghadiri, M. Electrostatic Enhancement of Coalescence of Water Droplets in Oil: A Review of the Technology. *Chem. Eng. J. (Amsterdam, Neth.)* **2002**, *85*, 357–368.

- (4) Zhang, Y.; Liu, Y.; Ji, R.; Wang, F.; Cai, B.; Li, H. Application of Variable Frequency Technique on Electrical Dehydration of Water-in-Oil Emulsion. *Colloids Surf, A* **2011**, *386*, 185–190.
- (5) He, L.; Yang, D.; Gong, R.; Ye, T.; Lü, Y.; Luo, X. An Investigation into the Deformation, Movement and Coalescence Characteristics of Water-in-Oil Droplets in an ac Electric Field. *Pet. Sci.* **2013**, *10*, 548–561.
- (6) Guo, C.; He, L. Coalescence Behaviour of Two Large Water-Drops in Viscous Oil under a dc Electric Field. *J. Electrost.* **2014**, *72*, 470–476.
- (7) Taylor, G. Disintegration of Water Drops in an Electric Field. *Proc. R. Soc. London, Ser. A* **1964**, *280*, 383–397.
- (8) Dubash, N.; Mestel, A. J. Behaviour of a Conducting Drop in a Highly Viscous Fluid Subject to an Electric Field. *J. Fluid Mech.* **2007**, *581*, 469–493.
- (9) Dubash, N.; Mestel, A. J. Breakup Behavior of a Conducting Drop Suspended in a Viscous Fluid Subject to an Electric Field. *Phys. Fluids* **2007**, *19*, 1–13.
- (10) Ha, J. W.; Yang, S. M. Deformation and Breakup of Newtonian and Non-Newtonian Conducting Drops in an Electric Field. *J. Fluid Mech.* **2000**, *405*, 131–156.
- (11) Vizika, O.; Saville, D. A. The Electrohydrodynamic Deformation of Drops Suspended in Liquids in Steady and Oscillatory Electric Fields. *J. Fluid Mech.* **1992**, *239*, 1–21.
- (12) Moriya, S.; Adachi, K.; Kotaka, T. Deformation of Droplets Suspended in Viscous Media in an Electric Field. 1: Rate of Deformation. *Langmuir* **1986**, *2*, 155–160.
- (13) Karyappa, R. B.; Deshmukh, S. D.; Thaokar, R. M. Breakup of a Conducting Drop in a Uniform Electric Field. *J. Fluid Mech.* **2014**, *754*, 550–589.
- (14) Eow, J. S.; Ghadiri, M. Motion, Deformation and Break-up of Aqueous Drops in Oils under High Electric Field Strength. *Chem. Eng. Process.* **2003**, *42*, 259–272.
- (15) Wright, G. S.; Krein, P. T.; Chato, J. C. Self-consistent Modeling of the Electrohydrodynamics of a Conductive Meniscus. *IEEE Trans. Ind. Appl.* **1995**, *31*, 768–777.
- (16) Nishiwaki, T.; Adachi, K.; Kotaka, T. Deformation of Viscous Droplets in an Electric Field: Poly (propylene oxide)/Poly (dimethylsiloxane) Systems. *Langmuir* **1988**, *4*, 170–175.
- (17) Ye, T. Motion and Coalescence Micro-Characteristics of Drops in Electrostatic Field. M.S. Dissertation, China University of Petroleum, Qingdao, 2010.
- (18) Torza, S.; Cox, R. G.; Mason, S. G. Electrohydrodynamic Deformation and Burst of Liquid Drops. *Philos. Trans. R. Soc., A* **1971**, *269*, 295–319.
- (19) Taylor, S. E. Investigations into the Electrical and Coalescence Behaviour of Water-in-Crude Oil Emulsions in High Voltage Gradients. *Colloids Surf.* **1988**, *29*, 29–51.
- (20) Zhang, J.; Dong, S.; Gan, Q. Dynamic Model of Liquid Droplets of Water in Oil Emulsion with High Frequency Pulsating Electric Field. *Huagong Xuebao (Chin. Ed.)* **2007**, *58*, 875–880.
- (21) Gong, H.; Peng, Y.; Shang, H.; Yang, Z.; Zhang, X. Non-Linear Vibration of a Water Drop Subjected to High-Voltage Pulsed Electric Field in Oil: Estimation of Stretching Deformation and Resonance Frequency. *Chem. Eng. Sci.* **2015**, *128*, 21–27.
- (22) Sherwood, J. D. Breakup of Fluid Droplets in Electric and Magnetic Fields. *J. Fluid Mech.* **1988**, *188*, 133–146.
- (23) Basaran, O. A.; Patzek, T. W.; Benner, R. E., Jr; Scriven, L. E. Nonlinear Oscillations and Breakup of Conducting, Inviscid Drops in an Externally Applied Electric Field. *Ind. Eng. Chem. Res.* **1995**, *34*, 3454–3465.
- (24) Yeo, L. Y.; Lastochkin, D.; Wang, S. C.; Chang, H. C. A New ac Electrospray Mechanism by Maxwell-Wagner Polarization and Capillary Resonance. *Phys. Rev. Lett.* **2004**, *92*, 133902–1.
- (25) Berg, G.; Lundgaard, L. E.; Abi-Chebel, N. Electrically Stressed Water Drops in Oil. *Chem. Eng. Process.* **2010**, *49*, 1229–1240.
- (26) Deng, W.; Gomez, A. Full Transient Response of Taylor Cones to a Step Change in Electric Field. *Microfluid. Nanofluid.* **2012**, *12*, 383–393.
- (27) Raisin, J.; Atten, P.; Reboud, J. L. A Novel Actuation Technique for the On-demand Injection of Charge-free Conducting Droplets in a Viscous Dielectric Liquid. *Exp. Fluids* **2013**, *54*, 1–14.
- (28) Yan, H.; He, L.; Luo, X.; Wang, J. The Study of Deformation Characteristics of Polymer Droplet under Electric Field. *Colloid Polym. Sci.* [Online early access]. Doi: 10.1007/s00396-015-3597-5, published online: Apr. 25, 2015. <http://link.springer.com/article/10.1007/s00396-015-3597-5>; (accessed Apr. 25, 2015).
- (29) Feng, J. T.; Zhao, Y. P. Experimental Observation of Electrical Instability of Droplets on Dielectric Layer. *J. Phys. D: Appl. Phys.* **2008**, *41*, 052004.
- (30) James Sir, J. *Mathematical Theory of Electricity and Magnetism*, 5th ed.; Cambridge University Press: Cambridge, U.K., 1966; p 153.